Circulation
JOURNAL OF THE AMERICAN HEART ASSOCIATION

American Heart Association®
Learn and Live℠

Three-Dimensional Electroanatomic Voltage Mapping Increases Accuracy of Diagnosing Arrhythmogenic Right Ventricular Cardiomyopathy/Dysplasia

Domenico Corrado, Cristina Basso, Loira Leoni, Barbara Tokajuk, Barbara Bauce, Gianfranco Frigo, Giuseppe Tarantini, Massimo Napodano, Pietro Turrini, Angelo Ramondo, Luciano Daliento, Andrea Nava, Gianfranco Buja, Sabino Iliceto and Gaetano Thiene

Circulation 2005, 111:3042-3050: originally published online June 6, 2005
doi: 10.1161/CIRCULATIONAHA.104.486977
Circulation is published by the American Heart Association. 7272 Greenville Avenue, Dallas, TX 72514
Copyright © 2005 American Heart Association. All rights reserved. Print ISSN: 0009-7322. Online ISSN: 1524-4539

The online version of this article, along with updated information and services, is located on the World Wide Web at:
http://circ.ahajournals.org/content/111/23/3042

Subscriptions: Information about subscribing to Circulation is online at
http://circ.ahajournals.org//subscriptions/

Permissions: Permissions & Rights Desk, Lippincott Williams & Wilkins, a division of Wolters Kluwer Health, 351 West Camden Street, Baltimore, MD 21202-2436. Phone: 410-528-4050. Fax: 410-528-8550. E-mail:
journalpermissions@lww.com

Reprints: Information about reprints can be found online at
http://www.lww.com/reprints

Downloaded from http://circ.ahajournals.org/ by guest on July 29, 2011

Three-Dimensional Electroanatomic Voltage Mapping Increases Accuracy of Diagnosing Arrhythmogenic Right Ventricular Cardiomyopathy/Dysplasia

Domenico Corrado, MD, PhD; Cristina Basso, MD, PhD; Loira Leoni, MD; Barbara Tokajuk, MD; Barbara Bauce, MD, PhD; Gianfranco Frigo, MD; Giuseppe Tarantini, MD; Massimo Napodano, MD; Pietro Turrini, MD, PhD; Angelo Ramondo, MD; Luciano Daliento, MD; Andrea Nava, MD; Gianfranco Buja, MD; Sabino Iliceto, MD; Gaetano Thiene, MD

Background—Three-dimensional electroanatomic voltage mapping offers the potential to identify low-voltage areas that correspond to regions of right ventricular (RV) myocardial loss and fibrofatty replacement in patients with arrhythmogenic RV cardiomyopathy/dysplasia (ARVC/D).

Methods and Results—Thirty-one consecutive patients (22 men and 9 women; mean age, 30.8±7 years) who fulfilled the criteria of the Task Force of the European Society of Cardiology and International Society and Federation of Cardiology (ESC/ISFC) for ARVC/D diagnosis after noninvasive clinical evaluation underwent further invasive study including RV electroanatomic voltage mapping and endomyocardial biopsy (EMB) to validate the diagnosis. Multiple RV endocardial, bipolar electrograms (175±23) were sampled during sinus rhythm. Twenty patients (group A; 65%) had an abnormal RV electroanatomic voltage mapping showing ≥1 area (mean 2.25±0.7) with low-voltage values (bipolar electrogram amplitude <0.5 mV), surrounded by a border zone (0.5 to 1.5 mV) that transitioned into normal myocardium (>1.5 mV). Low-voltage electrograms appeared fractionated with significantly prolonged duration and delayed activation. In 11 patients (group B; 35%), electroanatomic voltage mapping was normal, with preserved electrogram voltage (4.4±0.7 mV) and duration (37.2±0.9 ms) throughout the RV. Low-voltage areas in patients from group A corresponded to echocardiographic/angiographic RV wall motion abnormalities and were significantly associated with myocyte loss and fibrofatty replacement at EMB ($P<0.0001$) and familial ARVC/D ($P<0.0001$). Patients from group B had sporadic disease and histopathological evidence of inflammatory cardiomyopathy ($P<0.0001$). During the time interval from onset of symptoms to the invasive study, 11 patients (55%) with electroanatomic low-voltage regions received an implantable cardioverter/defibrillator because of life-threatening ventricular arrhythmias, whereas all but 1 patient with a normal voltage map remained stable on antiarrhythmic drug therapy ($P=0.02$).

Conclusions—Three-dimensional electroanatomic voltage mapping enhanced accuracy for diagnosing ARVC/D (1) by demonstrating low-voltage areas that were associated with fibrofatty myocardial replacement and (2) by identifying a subset of patients who fulfilled ESC/ISFC Task Force diagnostic criteria but showed a preserved electrogram voltage, an inflammatory cardiomyopathy mimicking ARVC/D, and a better arrhythmic outcome. (***Circulation*. 2005;111:3042-3050.)**

Key Words: cardiomyopathy ■ death, sudden ■ electrophysiology ■ mapping ■ myocarditis

Arrhythmogenic right ventricular cardiomyopathy/dysplasia (ARVC/D) is a heart muscle disease, often familial, that is characterized pathologically by RV myocardial atrophy with fibrofatty replacement and clinically by peculiar RV electric instability predisposing to life-threatening ventricular arrhythmias and sudden death.[1–6] At this stage of knowledge, molecular diagnosis of ARVC/D is not feasible in the majority of cases because of a large genetic heterogeneity and limitation of screening to the few genes discovered thus far.[7–11] Clinical diagnosis may be difficult because of several problems with the specificity of ECG abnormalities, with the different potential etiology of RV arrhythmias, and with the assessment of the RV structure and function by current imaging technique.[12–14]

Although MRI has the unique ability to characterize tissue, particularly discriminating fat from muscle, several limitations and a high degree of interobserver variability in the evaluation of RV free wall thinning and fatty infiltration have

Received June 23, 2004; revision received February 14, 2005; accepted March 2, 2005.

From the Division of Cardiology (D.C., L.L., B.T., B.B., G.T., M.N., G.F., P.T., A.R., L.D., A.N., G.B., S.I.) and Institute of Pathological Anatomy (C.B., G.T.), University of Padua Medical School, Padua, Italy.

Correspondence to Gaetano Thiene, MD, Istituto di Anatomia Patologica, Via A. Gabelli, 61-35121 Padova, Italy. E-mail cardpath@unipd.it

© 2005 American Heart Association, Inc.

Circulation **is available at http://www.circulationaha.org** **DOI: 10.1161/CIRCULATIONAHA.104.486977**

Downloaded from http://circ.ahajournals.org/ by guest on July 29, 2011

TABLE 1. Clinical Characteristics of Overall Sample and According to Results of Voltage Mapping

	Overall Sample (n=31)	Abnormal Voltage Mapping (Group A) (n=20)	Normal Voltage Mapping (Group B) (n=11)	P*
Age, y	30.8±7	30.5±12	31.3±9	0.23
Sex, male	22 (71)	14 (70)	8 (73)	0.80
Family history	13 (42)	13 (65)	0	<0.0001
Competitive athletes	12 (39)	7 (35)	5 (45)	0.85
Clinical symptoms	26 (84)	17 (85)	9 (82)	0.78
Cardiac arrest	2 (6)	2 (10)	0	0.52
Syncope	10 (32)	9 (45)	1 (9)	0.05
Palpitations	14 (45)	6 (30)	8 (73)	0.05
No symptoms	5 (16)	3 (15)	2 (18)	1.0
Antiarrhythmic drug therapy	28 (90)	19 (95)	9 (82)	0.58
Sotalol	11 (35)	7 (35)	4 (36)	1.00
Amiodarone	8 (26)	6 (30)	2 (18)	0.67
β-Blockers	6 (19)	4 (20)	2 (18)	1.00
Amiodarone+β-blockers	3 (10)	2 (10)	1 (9)	1.00
Interval between onset of symptoms and voltage map, mo	40.3±23	39±26	42±19	0.30

Values in parentheses are percentages.
*Comparison between group A and B.

been reported.[15,16] Therefore, a definitive phenotypic diagnosis of ARVC/D relies on the histopathological demonstration of fibrofatty substitution of the RV myocardium, either at postmortem or in vivo by endomyocardial biopsy (EMB).[2,4,5,17] This latter option, however, has diagnostic limitations related to the segmental nature of the disease and its inability to assess transmural changes of RV wall. Moreover, there may be difficulty in differentiating ARVC/D biopsy findings from either the normal amount of subepicardial adipose tissue or other cardiomyopathy/myocarditis.[14]

Three-dimensional electroanatomic voltage mapping has been recently demonstrated to accurately identify the presence, location, and extent of the pathological substrate of ARVC/D by detection of low-voltage regions that reflect RV fibrofatty myocardial atrophy.[18]

The present study was designed to test whether characterization of the RV wall by electroanatomic voltage mapping increases the accuracy for diagnosing ARVC/D in a consecutive series of patients fulfilling noninvasive Task Force criteria.

Methods

The study comprised 31 patients (22 men and 9 women; mean age, 30.8±7 years). Clinical characteristics are reported in Tables 1 and 2.

Noninvasive Study

Noninvasive evaluation in all patients included history, physical examination, laboratory tests, chest radiograph, 12-lead ECG recording, 24-hour Holter monitoring, signal-averaged ECG, exercise stress testing, and 2D and color Doppler echocardiography. Technical equipment, protocols, and reference values of each investigation have been reported in detail elsewhere.[6] ARVC/D cases were considered "familial" on the basis of pedigree analysis showing other affected individuals or premature (<40 years) sudden deaths by family history and noninvasive clinical screening of nuclear family members. In the absence of another family member with ARVC/D or with sudden death, the disease was defined as "sporadic." After noninvasive study, all patients fulfilled criteria for diagnosis of ARVC/D as recommended by the European Society of Cardiology and International Society and Federation of Cardiology (ESC/ISFC) Task Force.[12,13]

Invasive Study

All patients underwent invasive study that included left and RV cineangiography (in the right and left anterior oblique views) and coronary angiography as previously reported,[19] EMB, and 3D electroanatomic voltage mapping. An electrophysiological study with programmed ventricular stimulation was performed in 20 patients (65%) clinically presenting with life-threatening ventricular tachyarrhythmias, syncope, or strong family history of sudden death. The study was approved by the institutional review board, and all patients gave their informed consent.

Endomyocardial Biopsy

EMB of the RV was obtained via the femoral vein with the use of the long sheath technique (disposable Cordis bioptome) in all patients. The samples were obtained at the junction between the ventricular septum and the anterior RV free wall. Three to 5 biopsy specimens (mean, 3.4) were obtained from each patient, fixed in 10% phosphate-buffered formalin (pH 7.35), and then processed for histological examination. Seven-micrometer-thick paraffin-embedded sections were serially cut and stained according to the hematoxylin-eosin and Heidenhain trichrome techniques. Histopathological diagnosis of ARVC/D was made independently by 2 observers (C.B, G.T.), blinded to voltage mapping results on the basis of a significant amount of fibrofatty myocardial atrophy with residual myocyte <45%, evaluated by histomorphometric analysis.[17] Dallas criteria were used for histological diagnosis of myocarditis.[20] To characterize cellular infiltrates, additional paraffin-embedded tissue sections were stained with a panel of monoclonal antibodies according to the avidin-biotin peroxidase complex method (Vector). Agreement of interobserver analysis was 94%, and discrepancies were resolved by consensus.

Downloaded from http://circ.ahajournals.org/ by guest on July 29, 2011

TABLE 2. Instrumental Findings of Overall Sample and According to Results of Voltage Mapping

	Overall Sample (n=31)	Abnormal Voltage Mapping (Group A) (n=20)	Normal Voltage Mapping (Group B) (n=11)	P*
Depolarization/conduction ECG abnormalities				
"Epsilon wave" in V1-V2/V3	4 (13)	4 (20)	0	0.26
QRS amplitude ≤0.5 mV in limb leads	8 (26)	8 (40)	0	0.03
Right precordial QRS duration ≥110 ms	18 (58)	16 (80)	2 (18)	0.003
Late potential on signal-averaged ECG	15 (48)	13 (65)	2 (18)	0.03
Repolarization ECG abnormalities	28 (90)	18 (90)	10 (91)	0.58
Inverted T waves beyond V1				
Ventricular arrhythmias				
Sustained ventricular tachycardia	15 (48)	9 (45)	6 (55)	0.89
Nonsustained ventricular tachycardia	12 (39)	8 (40)	4 (36)	1.00
Frequent premature ventricular beats	4 (13)	3 (15)	1 (9)	1.00
Structural/functional abnormalities†				
Global RV dilatation/dysfunction	23 (74)	15 (75)	8 (73)	0.77
RV wall motion abnormalities	25 (81)	18 (90)	7 (64)	0.19
Angiographic RV ejection fraction, %	47.9±7	47.2±8	48.3±9	0.45
Angiographic RV end-diastolic volume, mL/m^2	110±18	109±17	111±20	0.24
LV dilatation/dysfunction and/or regional hypo-akinesia	16 (52)	9 (45)	7 (64)	0.54
Endomyocardial biopsy findings				
ARVC/D	15 (48)	15 (75)	0	<0.0001
Inflammatory cardiomyopathy	10 (32)	0	10 (91)	<0.0001
Normal	6 (19)	5 (25)	1 (9)	0.38
Programmed ventricular stimulation	11/20 (55)	9/13 (69)	2/7 (28)	0.16
Inducible ventricular tachycardia	8/20 (40)	7/13 (54)	1/7 (14)	0.15
Inducible ventricular fibrillation	3/20 (15)	2/13 (15)	1/7 (14)	1.00
ICD therapy	12 (39)	11 (55)	1 (9)	0.02

Values in parentheses are percentages. LV indicates left ventricular; ICD, implantable cardioverter/defibrillator.
*Comparison between group A and B.
†Assessed by echocardiography/angiography.

According to the definition and classification of cardiomyopathies of the World Health Organization/ISFC Task Force, inflammatory cardiomyopathy was defined as myocarditis with cardiac dysfunction.[21]

Electroanatomic Voltage Mapping

All patients underwent 3D electroanatomic voltage mapping technique by the CARTO system (Biosense-Webster) during sinus rhythm, as previously reported.[22–30] In brief, the magnetic mapping system includes a magnetic sensor in the catheter tip that can be localized in 3D space with the ultralow magnetic field generators placed under the fluoroscopic table. A 7F Navi-Star catheter, which consisted of a 4-mm distal tip electrode and a 2-mm ring electrode with an interelectrode distance of 1 mm, was introduced into the RV under fluoroscopic guidance and used as the mapping catheter. The catheter was placed at multiple sites on the endocardial surface to record bipolar electrograms from RV inflow, anterior free wall, apex, and outflow. The bipolar signals were filtered at 10 to 400 Hz and were displayed at 100-mm/s speeds on the CARTO system. Bipolar electrograms were analyzed with regard to amplitude, duration, relation to the surface QRS, and presence of multiple components. The initial mapping points were sampled under fluoroscopic guidance to provide the outliers of the RV chamber geometry; thereafter, the mapping catheter was manipulated primarily by the CARTO system with fluoroscopy used only secondarily (mean, 9±1.2 minutes). A recording was accepted and integrated in the map when the variability in cycle length, local activation time stability, and maximum beat-to-beat difference of the location of the catheter were <2%, <3 ms, and <4 mm, respectively.[26] These parameters, combined with impedence measurements, were used to exclude signals with low amplitude due to poor endocardial catheter contact. In addition, adequate catheter contact was confirmed by concordant catheter tip motion with the cardiac silhouettes on fluoroscopy. The peak-to-peak signal amplitude of the bipolar electrogram was measured automatically. A 3D geometry of the RV chamber depicting the peak-to-peak amplitude of the bipolar electrograms recorded at each site was constructed in real time with the electrophysiological information color coded and superimposed on the reconstruction. Mapping points were acquired until a complete electroanatomic map of the RV had been generated. The voltage maps were edited, and intracavitary points, which were identified as sites located at abrupt indentations on the endocardial contour with associated sudden reduction in electrogram amplitudes compared with signals from surrounding sites, were eliminated.

Reference values were established by mapping the RV in 6 patients (5 men and 1 woman, aged 28±6 years) without structural heart disease who underwent electrophysiological study for evaluation of supraventricular tachycardia. None of these subjects was taking cardioactive drugs. A mean of 168±27 sites were recorded per normal RV. Electrograms recorded from all RV regions and septum were sharp, with single and rapid deflection, and showed a mean duration of 36.6±0.7 ms. The mean bipolar amplitude of the electrogram was 5.3±0.9 mV (range, 0.9 to 12.1 mV), with 95% of all electrogram signals >1.47 mV. Therefore, in this study the

Downloaded from http://circ.ahajournals.org/ by guest on July 29, 2011

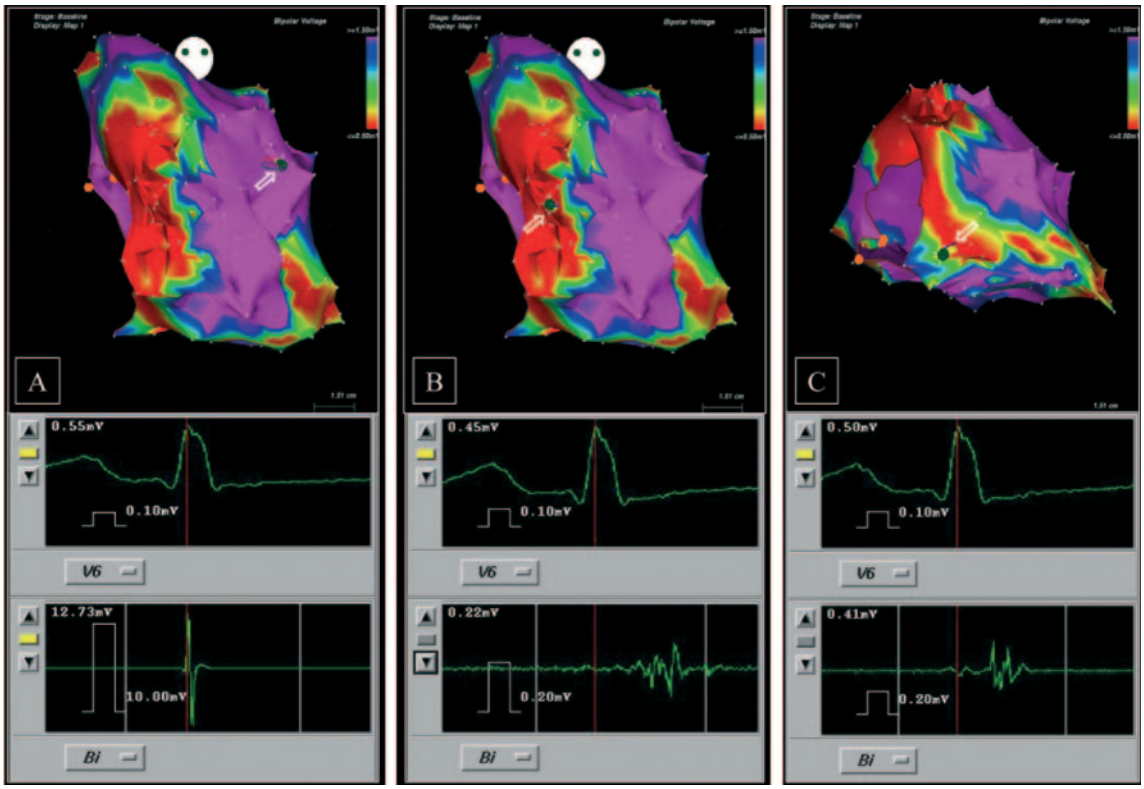

Figure 1. Abnormal 3D electroanatomic RV voltage map in both anteroposterior (A and B) and bottom (C) views, with examples of electric signals sampled from within normal and low-amplitude RV areas in the same patient with ARVC/D. Voltages are color coded according to corresponding color bars: purple represents signal amplitudes >1.5 mV (electroanatomic normal myocardium); red, <0.5 mV (electroanatomic scar tissue); and the range between purple and red, 0.5 to 1.5 mV (electroanatomic border zone). As indicated by the catheter tip (arrows), normal voltage electrogram sampled from the anterolateral region is sharp, biphasic deflection with large amplitude and short duration (A). By comparison, low-voltage electrograms recorded from anterior and inferobasal regions are fragmented with prolonged duration and late activation.

reference value for electrogram amplitude used to define normal RV endocardium was set at 1.5 mV, which was the value above which 95% of all bipolar signal voltages from the endocardium of normal RVs were included. According to previous experiences on intraoperative[30] and catheter mapping,[24,25,28–31] "electroanatomic scar" area was defined as an area ≥1 cm^2 including at least 3 adjacent points with bipolar signal amplitude <0.5 mV. The color display for depicting normal and abnormal voltage myocardium ranged from red, representing electroanatomic scar tissue (amplitude <0.5 mV), to purple, representing electroanatomic normal tissue (amplitude ≥1.5 mV). Intermediate colors represented the electroanatomic border zone (signal amplitudes between 0.5 and 1.5 mV) (Figures 1 to 3). Regions showing low-amplitude electrograms were mapped with greater point density to delineate the extent and borders of electroanatomic scar areas.

The concordance between location of low-voltage areas and RV wall motion abnormalities was assessed in each patient by a comparison of electroanatomic bipolar voltage mapping and echocardiographic/angiographic imaging by 3 blinded observers (D.C., B.B., L.D.). According to a previously reported protocol,[6,19] ventricular wall motion abnormalities were analyzed qualitatively by 2 observers blinded to voltage maps. Interobserver discrepancies were resolved by consensus.

Electrophysiological Study

All antiarrhythmic drugs were discontinued 5 half-lives (6 weeks for amiodarone) before the study. Programmed ventricular stimulation protocol included 3 drive-cycle lengths (600, 500, and 400 ms) and 3 ventricular extrastimuli while pacing from 2 RV sites (apex and outflow tract). Programmed ventricular stimulation was considered positive if either a ventricular fibrillation or a sustained ventricular tachycardia, ie, one that lasted ≥30 seconds or required termination because of hemodynamic compromise, was induced.

Statistical Analysis

Continuous variables are expressed as range and mean±SD. Categorical differences between groups were evaluated by Fisher exact text or χ^2 test. Differences between group means were compared by unpaired t test. All probability values reported are 2 sided, and a probability value <0.05 was considered statistically significant. SAS software (SAS Institute) was used for statistical analysis.

Results

Clinical characteristics and instrumental findings are summarized in Tables 1 and 2. The study population included 31 consecutive patients (22 men and 9 women; age range, 19 to 57 years; mean age, 30.8±7 years). Thirteen patients had a family history of ARVC/D or of premature (<40 years) sudden death due to proven or suspected ARVC/D. Five patients remained asymptomatic, whereas the remaining 26 had arrhythmia-related symptoms. Structural and functional RV abnormalities were observed at echocardiography/angiography in all patients. Wall motion abnormalities of the RV free wall were documented in 25 patients and affected ≥1 of the following RV regions: anterior in 17 patients, inferobasal in 13, inferior in 8, anteroapical in 7, infundibular in 7, lateral in 6, and inferoapical in 3. Ventricular arrhythmias were documented in all patients and included sustained

Downloaded from http://circ.ahajournals.org/ by guest on July 29, 2011

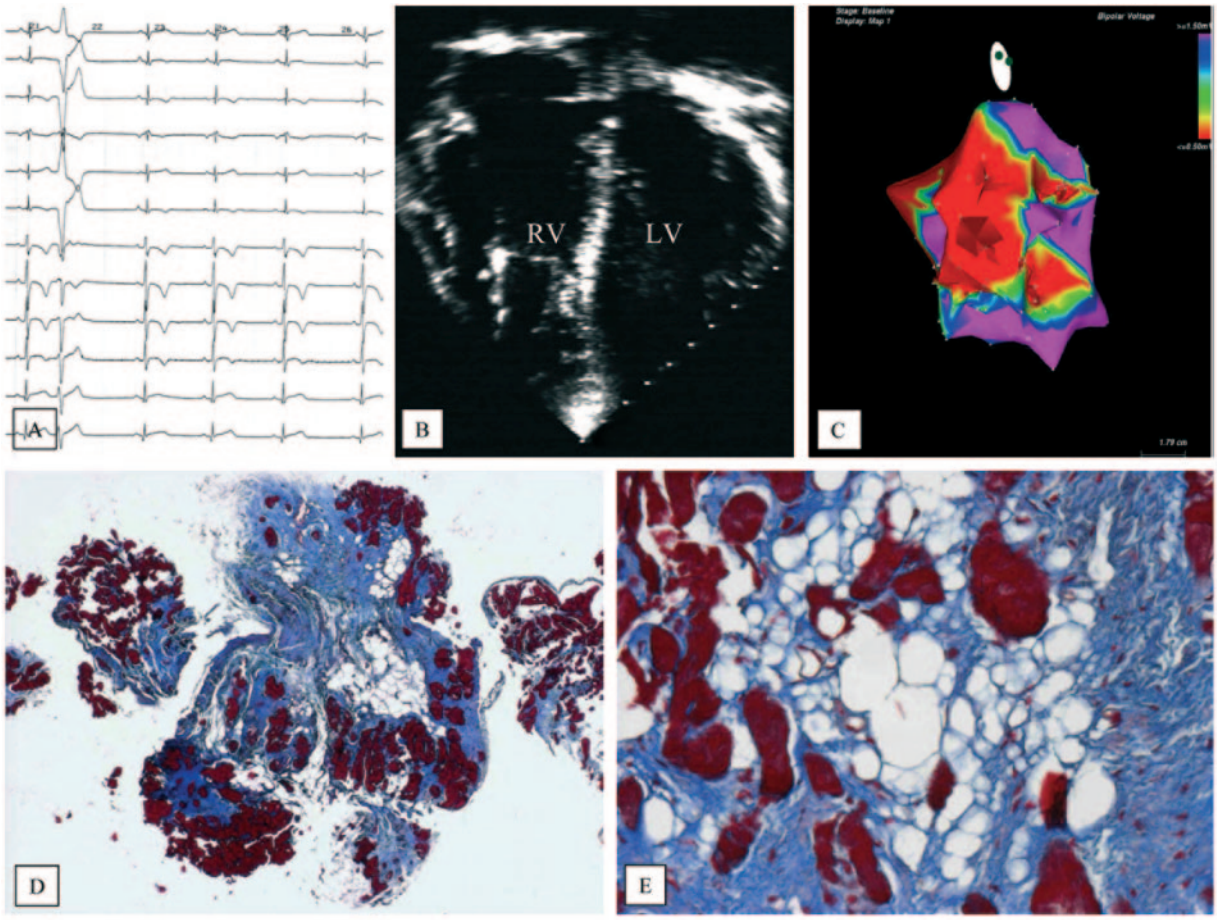

Figure 2. Noninvasive and invasive findings in a representative patient with abnormal RV electroanatomic voltage map. A, Twelve-lead ECG showing inverted T waves from V1 to V4 and a premature ventricular beat with a left bundle branch block/superior axis morphology. B, Two-dimensional echocardiographic apical view showing severe RV dilatation. C, Right anterior oblique view of RV bipolar voltage map showing low-voltage values (red indicates <0.5 mV) in anteroinfundibular, inferobasal, and apical regions. D, EMB sample showing massive myocardial atrophy and fibrofatty replacement (trichrome; magnification ×6). E, Close-up showing residual myocytes entrapped within fibrous and fatty tissue (trichrome; magnification ×40).

monomorphic ventricular tachycardia in 15, nonsustained ventricular tachycardia in 12, and frequent premature ventricular beats in 4. All types of ventricular arrhythmias showed a left bundle branch pattern with a superior axis in 14 cases, inferior axis in 11, and undetermined axis in 6. Eleven of the 20 patients (55%) undergoing electrophysiological study were inducible at programmed ventricular stimulation to either sustained monomorphic ventricular tachycardia (8 patients) or ventricular fibrillation (3 patients). The time interval from onset of symptoms to the invasive study including electroanatomic voltage mapping ranged from 7 to 75 months (mean, 40.3±23 months).

Endomyocardial Biopsy

In 15 patients, histological analysis of EMB samples demonstrated a diagnostic amount of myocardial atrophy and fibrofatty replacement (Figure 2), confirming the diagnosis of ARVC/D.

Of the remaining 16 patients, 6 were normal, and 10 had EMB histopathological changes that were consistent with the diagnosis of inflammatory cardiomyopathy (Figure 3). In 7 of these latter 10 patients, there were associated myocyte nuclear/cytological changes and interstitial and/or focal replacement fibrosis (Figure 3). The inflammatory infiltrates mainly consisted of activated T lymphocytes (CD45, CD45RO+, and CD43), with a few macrophages (CD68+) (Figure 3). No patients showed histological features of granulomatous and/or giant cell myocarditis.

Electroanatomic Voltage Mapping

The mean number of sites sampled in RV electroanatomic mapping was 175±23, with an average mapping period of 27±6 minutes. Twenty of 31 patients (65%) had an abnormal RV electroanatomic voltage mapping (group A) showing ≥1 area (mean, 2.25±0.7), including contiguous bipolar electrograms with voltage values <0.5 mV (ie, electronatomic scar tissue). Low-voltage areas were sharply demarcated and typically surrounded by a border zone with reduced signal amplitudes (0.5 to 1.5 mV), which merged into normal myocardium (>1.5 mV). Examples of abnormal RV voltage maps are shown in Figures 1 and 2. The most frequently involved RV regions were anterior in 13 patients, inferobasal in 12, infundibular in 6, anteroapical in 5, lateral in 4, inferior in 3, and inferoapical in 2. Seventeen patients showed a

Downloaded from http://circ.ahajournals.org/ by guest on July 29, 2011

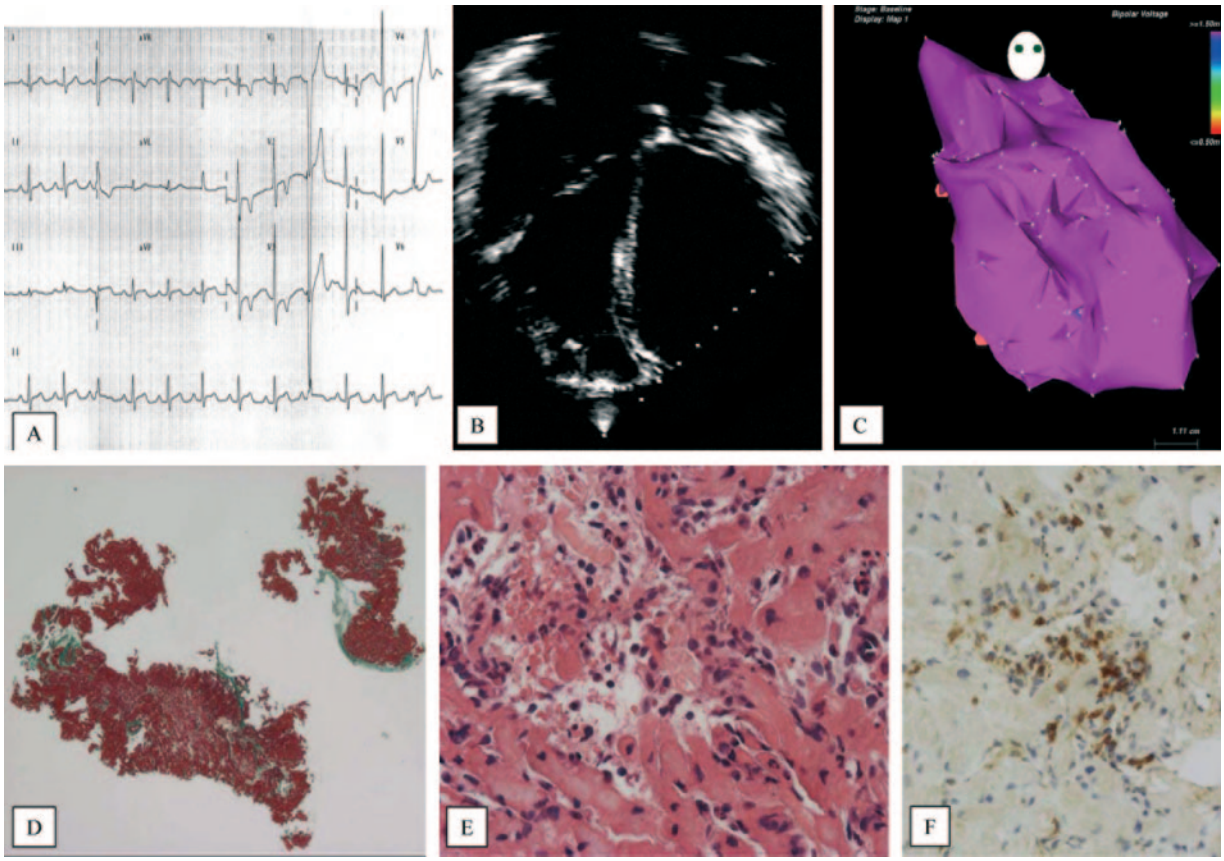

Figure 3. Noninvasive and invasive findings in a representative patient with normal RV electroanatomic voltage map. A, Twelve-lead ECG showing inverted T waves from V1 to V4 and a premature ventricular beat with a left bundle branch block morphology. B, Two-dimensional echocardiographic apical view showing severe RV dilatation. C, Right anterior oblique view of RV bipolar voltage map showing preserved bipolar voltages values (purple indicates >1.5 mV) throughout the RV. D, EMB samples showing mild interstitial and endocardial fibrosis (trichrome; magnification ×6). E, At higher magnification, inflammatory infiltrates and myocyte necrosis are visible (hematoxylin-eosin; magnification ×60). F, At immunohistochemistry, inflammatory cells mainly consist of T lymphocytes (CD43; magnification ×60).

widespread RV disease with demonstration of electroanatomic scar tissue in ≥2 RV regions, whereas 3 patients had a localized RV disease with segmental involvement of the inferobasal (2 patients) and infundibular (1 patient) RV free wall. The septum was spared in all but 2 patients, both showing a selective involvement of the apical region. Compared with electrograms sampled from unaffected areas, those recorded from within electroanatomic scar tissue showed significantly lower amplitude (0.4±0.08 versus 4.9±0.4 mV; $P<0.001$) and prolonged duration (77.2±21 versus 35.8±6.3 ms; $P<0.001$) and also significantly more often appeared to be fragmented (79%; $P<0.001$) and extended beyond the offset of the surface QRS (61%; $P<0.001$) (Figure 1B, 1C).

In the remaining 11 patients (35%), electroanatomic voltage mappings were normal (group B), with preserved bipolar electrogram amplitude (4.4±0.7 mV) and duration (37.2±0.9) throughout the RV free wall and septum (Figure 3C).

Correlation of Results

Compared with patients from group B, those from group A significantly more often had a positive family history for ARVC/D or sudden death ($P<0.0001$), fibrofatty myocardial replacement at EMB ($P<0.0001$), depolarization/conduction ECG abnormalities such as low-voltage QRS in limb leads ($P=0.03$), right precordial QRS duration ≥110 ms ($P=0.003$), and late potentials at signal-averaged ECG ($P=0.03$); syncopal episodes, either unexplained or caused by sustained ventricular tachycardia, and palpitations reached only borderline statistical significance ($P=0.05$) (Tables 1 and 2).

A concordance between the location of electroanatomic low-voltage areas and akinetic/dyskinetic regions at echocardiography/angiography was found in all but 2 patients in whom electroanatomic low-amplitude areas involving the RV inflow portion had been missed at wall motion analysis by echocardiography/angiography.

Patients from group B distinctively had nonfamilial disease ($P<0.0001$) and significantly more often showed histopathological evidence of inflammatory cardiomyopathy ($P<0.0001$). Eleven patients (55%) from group A received an implantable cardioverter/defibrillator because of either ventricular tachyarrhythmias associated with hemodynamic compromise or unexplained syncopal episodes, whereas all but 1 patient from group B remained stable on antiarrhythmic therapy ($P=0.02$).

Downloaded from http://circ.ahajournals.org/ by guest on July 29, 2011

Discussion

The major finding of the present study was that 3D electroanatomic RV voltage mapping in ARVC/D demonstrated low-voltage areas that correlated with myocardial loss and fibrofatty replacement at EMB and identified a subset of patients who fulfilled electrocardiographic and echocardiographic Task Force diagnostic criteria but showed normal electroanatomic mapping findings, an inflammatory cardiomyopathy mimicking ARVC/D, and a better arrhythmic outcome.

Abnormal Electroanatomic Voltage Mapping

The finding of significant loss of myocardium resulting in the recording of low-amplitude, fractionated endocardial electrograms has been previously well established in patients with either ischemic or nonischemic ventricular scar by intraoperative mapping,[30] conventional endocardial mapping,[31] and 3D electroanatomic mapping technique.[18,27–29]

The hallmark pathological lesion of ARVC/D is a transmural loss of the myocardium with replacement by fibrofatty tissue of the RV free wall, accounting for variable degree of RV wall thinning, with areas so thin as to appear completely devoid of muscle at transillumination.[2,4,5,32] The present study confirms and extends previous observations by showing that electroanatomic voltage mapping has the ability to identify areas of myocardial atrophy by recording and spatially associating low-amplitude electrograms to generate a 3D electroanatomic map of the RV chamber. The electroanatomic low-amplitude areas were significantly associated with the histopathological finding of myocyte loss and fibrofatty replacement at EMB, thus confirming that RV loss of voltage reflects the replacement of action potential–generating myocardial tissue with electrically silent fibrofatty tissue. A sampling error of EMB due to segmental RV involvement may explain the apparently normal findings obtained in 5 patients of group A, 3 of whom showed low-voltage values limited to a single RV region.

There was a concordance between the presence and location of RV low-voltage areas identified by electroanatomic map and akinetic/dyskinetic regions detected by echocardiography and/or angiography. The low-amplitude electrogram values were distinctively recorded in the RV free wall, predominantly involving the anterolateral, infundibular, and inferobasal regions, and spared the interventricular septum. Such a spatial distribution is similar to that observed in autopsy hearts of patients who died from ARVC/D, in whom the most severe RV myocardial atrophy and wall aneurysms are mostly localized in the anteroinfundibular free wall and underneath the tricuspid valve.[4,5,32]

In the present study the majority of patients with an abnormal electroanatomic voltage mapping had a familial form of ARVC/D. This finding is in agreement with the genetic background of the disease, which has been demonstrated in >50% of ARVC/D patients with either the autosomal or, less frequently, the recessive pattern of inheritance and age-related and variable penetrance.[6–11]

Normal Electroanatomic Voltage Mapping

Thirty-five percent of patients who fulfilled the Task Force diagnostic criteria for ARVC/D at noninvasive evaluation showed neither evidence of electroanatomic low-voltage regions nor fibrofatty replacement at voltage mapping and EMB. Comparison of mapping results and clinical patient characteristics in the present study suggests that the finding of normal RV voltage values characterizes a distinct subgroup of patients with a peculiar etiopathogenetic, clinical, and prognostic profile.

Patients with normal and abnormal electroanatomic voltage mapping did not differ with regard to mean age and mean time interval between symptom onset and time of electroanatomic evaluation. Moreover, extent of precordial ECG repolarization changes and severity of morphofunctional abnormalities such as global or segmental RV dilatation/dysfunction, RV wall motion abnormalities, and left ventricular involvement, which were detected by echocardiography/angiography, were similar in both subgroups of patients. These findings argue against the possibility that failure to detect electroanatomic RV low-voltage areas reflects early stages or minor variants of ARVC/D.

All patients with a normal electroanatomic voltage mapping were sporadic cases, showing neither a familial history of sudden death nor evidence of familial ARVC/D at clinical screening of family members. Of importance, all but 1 patient showed EMB histopathological changes consistent with the diagnosis of inflammatory cardiomyopathy.

Chronic myocarditis mimicking ARVC/D has been previously reported in nonfamilial patients.[33,34] In the majority of our patients, the association between inflammatory changes and focal fibrosis suggested a longstanding disease with either a persistent or recurrent myocardial inflammatory process at different stages of healing. Although such a patchy fibrosis is frequently observed in patients with inflammatory cardiomyopathy, extensive and transmural areas of myocardial depletion with scarring are noted exceptionally,[35] thus explaining the absence of low-voltage areas.

Involvement of ventricular myocardium by sarcoid may also mimic ARVC/D.[36] In our study cardiac sarcoidosis was ruled out by EMB histological findings that did not show any suggestive well-formed, nonnecrotizing inflammatory granulomas.

Study Limitations

Our study was limited by a small sample size that may have led to type II error for some clinical differences observed in the subgroup analysis. However, the population of patients with ARVC/D is also limited because of the low disease prevalence. We studied a selected patient population fulfilling the ESC/ISFC criteria for ARVC/D, and the study results may not be generalizable to patients affected by different heart muscle diseases causing scarring in the RV such as sarcoidosis, skeletal-muscle dystrophies, and other right-sided cardiomyopathies, either ischemic or nonischemic.

Clinical Implications and Conclusions

At least 30% of cases of dilated cardiomyopathy are familial and linked to genetic defects in "force transmission" proteins, whereas a significant percentage of the remaining sporadic cases recognizes a viral and/or immune myocarditis pathogenesis.[37] Similarly, the results of the present study indicate that ARVC/D includes both familial cases, characterized by a

Downloaded from http://circ.ahajournals.org/ by guest on July 29, 2011

distinctive loss of myocardium reflecting a genetically determined dystrophic process, and sporadic forms that in part may be the result of an inflammatory myocardial disease predominantly involving the RV. ESC/ISFC Task Force guidelines show significant limitations in specificity when used for diagnosing nonfamilial ARVC/D. There were sporadic cases who fulfilled diagnostic criteria for ARVC/D but showed negative voltage map findings in association with histopathological evidence of inflammatory cardiomyopathy. Such patients with RV inflammatory myocardial disease mimicking ARVC/D can be detected by an electroanatomic voltage map that rules out RV regions with loss of electrogram voltage.

The only noninvasive parameters significantly associated with electroanatomic low-voltage areas were right precordial QRS prolongation, low-voltage QRS in the limb leads, and late potentials. Accordingly, intracardiac electrograms recorded from within the electroanatomic RV low-voltage areas often appeared fractionated with a significantly prolonged duration and extended beyond the offset of the surface QRS compared with electrograms recorded from normal-voltage regions areas. All of these electric abnormalities, either surface or intracardiac, reflect the distinctive pathoarrhythmogenic substrate of ARVC/D, ie, a fibrofatty scar, which accounts for a right intraventricular conduction defect and predisposes to life-threatening ventricular arrhythmias.[38–40]

Abnormal electroanatomic voltage mapping was associated with a worse arrhythmic clinical course. During the time interval from onset of symptoms to the invasive study, 55% of patients with electroanatomic evidence of low-voltage areas required an implantable cardioverter/defibrillator because of serious arrhythmic complications, whereas all but 1 patient with preserved myocardial voltage values remained stable on antiarrhythmic therapy. The predictive accuracy of voltage mapping to identify those patients more prone to sudden death remains to be assessed by a prospective follow-up study.

Acknowledgments

This study was supported by European Community ARVC/D research contract QLG1 CT-2000 01091; Ministry of Health, Rome, Italy; and Fondazione Cassa di Risparmio Padova e Rovigo, Italy.

References

1. Marcus FI, Fontaine GH, Guiraudon G, Frank R, Laurenceau JL, Malergue C, Grosgogeat Y. Right ventricular dysplasia: a report of 24 adult cases. *Circulation*. 1982;65:384–398.
2. Thiene G, Nava A, Corrado D, Rossi L, Pennelli N. Right ventricular cardiomyopathy and sudden death in young people. *N Engl J Med*. 1988;318:129–133.
3. Corrado D, Basso C, Thiene G. Sudden death. In: Nava A, Rossi L, Thiene G, eds. *Arrhythmogenic Right Ventricular Cardiomyopathy/Dysplasia*. Amsterdam, Netherlands: Elsevier; 1997.
4. Basso C, Thiene G, Corrado D, Angelini A, Nava A, Valente M. Arrhythmogenic right ventricular cardiomyopathy: dysplasia, dystrophy, or myocarditis? *Circulation*. 1996;94:983–991.
5. Corrado D, Basso C, Thiene G, McKenna WJ, Davies MJ, Fontaliran F, Nava A, Silvestri F, Blomstrom-Lundqvist C, Wlodarska EK, Fontaine G, Camerini F. Spectrum of clinicopathologic manifestations of arrhythmogenic right ventricular cardiomyopathy/dysplasia: a multicenter study. *J Am Coll Cardiol*. 1997;30:1512–1520.
6. Nava A, Bauce B, Basso C, Muriago M, Rampazzo A, Villanova C, Daliento L, Buja G, Corrado D, Danieli GA, Thiene G. Clinical profile and long-term follow-up of 37 families with arrhythmogenic right ventricular cardiomyopathy. *J Am Coll Cardiol*. 2000;36:2226–2233.
7. McKoy G, Protonotarios N, Crosby A, Tsatsopoulou A, Anastasakis A, Coonar A, Norman M, Baboonian C, Jeffery S, McKenna WJ. Identification of a deletion in plakoglobin in arrhythmogenic right ventricular cardiomyopathy with palmoplantar keratoderma and woolly hair (Naxos disease). *Lancet*. 2000;355:2119–2124.
8. Tiso N, Stephan DA, Nava A, Bagattin A, Devaney JM, Stanchi F, Larderet G, Brahmbhatt B, Brown K, Bauce B, Muriago M, Basso C, Thiene G, Danieli GA, Rampazzo A. Identification of mutations in the cardiac ryanodine receptor gene in families affected with arrhythmogenic right ventricular cardiomyopathy type 2 (ARVD2). *Hum Mol Genet*. 2001;10:189–194.
9. Rampazzo A, Nava A, Malacrida S, Beffagna G, Bauce B, Rossi V, Zimbello R, Simionati B, Basso C, Thiene G, Towbin JA, Danieli GA. Mutation in human desmoplakin domain binding to plakoglobin causes a dominant form of arrhythmogenic right ventricular cardiomyopathy. *Am J Hum Genet*. 2002;71:1200–1206.
10. Beffagna G, Occhi G, Nava A, Vitiello L, Ditadi A, Basso C, Bauce B, Carraro G, Thiene G, Towbin JA, Danieli GA, Rampazzo A. Regulatory mutations in transforming growth factor-β3 gene cause arrhythmogenic right ventricular cardiomyopathy type 1. *Cardiovasc Res*. 2005;65:366–373.
11. Gerull B, Heuser A, Wichter T, Paul M, Basson CT, McDermott DA, Lerman BB, Markowitz SM, Ellinor PT, MacRae CA, Peters S, Grossmann KS, Drenckhahn J, Michely B, Sasse-Klaassen S, Birchmeier W, Dietz R, Breithardt G, Schulze-Bahr E, Thierfelder L. Mutations in the desmosomal protein plakophilin-2 are common in arrhythmogenic right ventricular cardiomyopathy. *Nat Genet*. 2004;36:1162–1164.
12. McKenna WJ, Thiene G, Nava A, Fontaliran F, Blomstrom-Lundqvist C, Fontaine G, Camerini F. Diagnosis of arrhythmogenic right ventricular dysplasia/cardiomyopathy. *Br Heart J*. 1994;71:215–218.
13. Corrado D, Fontaine G, Marcus FI, McKenna WJ, Nava A, Thiene G, Wichter T. Arrhythmogenic right ventricular dysplasia/cardiomyopathy: need for an international registry. *Circulation*. 2000;101:e101–e106.
14. Corrado D, Basso C, Thiene G. Arrhythmogenic right ventricular cardiomyopathy: diagnosis, prognosis, and treatment. *Heart*. 2000;83:588–595.
15. Bluemke DA, Krupinski EA, Ovitt T, Gear K, Unger E, Axel L, Boxt LM, Casolo G, Ferrari VA, Funaki B, Globits S, Higgins CB, Julsrud P, Lipton M, Mawson J, Nygren A, Pennell DJ, Stillman A, White RD, Wichter T, Marcus F. MR imaging of arrhythmogenic right ventricular cardiomyopathy: morphologic findings and interobserver reliability. *Cardiology*. 2003;99:153–162.
16. Bomma C, Rutberg J, Tandri H, Nasir K, Roguin A, Tichnell C, Rodriguez R, James C, Kasper E, Spevak P, Bluemke DA, Calkins H. Misdiagnosis of arrhythmogenic right ventricular dysplasia/cardiomyopathy. *J Cardiovasc Electrophysiol*. 2004;15:300–306.
17. Angelini A, Basso C, Nava A, Thiene G. Endomyocardia1 biopsy in arrhythmogenic right ventricular cardiomyopathy. *Am Heart J*. 1996;132:203–206.
18. Boulos M, Lashevsky I, Reisner S, Gepstein L. Electroanatomical mapping of arrhythmogenic right ventricular dysplasia. *J Am Coll Cardiol*. 2001;38:2020–2027.
19. Daliento L, Rizzoli G, Thiene G, Nava A, Rinuncini M, Chioin R, Dalla Volta S. Diagnostic accuracy of right ventriculography in arrhythmogenic right ventricular cardiomyopathy. *Am J Cardiol*. 1990;66:741–745.
20. Aretz HT, Billingham ME, Edwards WD, Factor SM, Fallon JT, Fenoglio JJ Jr, Olsen EG, Schoen FJ. Myocarditis: a histopathologic definition and classification. *Am J Cardiovasc Pathol*. 1987;1:3–14.
21. Richardson P, McKenna W, Bristow M, Maisch B, Mautner B, O'Connell J, Olsen E, Thiene G, Goodwin J, Gyarfas I, Martin I, Nordet P. Report of the 1995 WHO/ISFC Task Force on the definition and classification of cardiomyopathies. *Circulation*. 1996;93:841–842.
22. Ben-Haim SA, Osadchy D, Schuster I, Gepstein L, Hayam G, Josephson ME. Nonfluoroscopic, in vivo navigation and mapping technology. *Nat Med*. 1996;2:1393–1395.
23. Gepstein L, Hayam G, Ben-Haim SA. A novel method for nonfluoroscopic catheter-based electroanatomical mapping of the heart: in vitro and in vivo accuracy results. *Circulation*. 1997;95:1611–1622.
24. Gepstein L, Goldin A, Lessick J, Hayam G, Shpun S, Schwartz Y, Hakim G, Shofty R, Turgeman A, Kirshenbaum D, Ben-Haim SA. Electromechanical characterization of chronic myocardial infarction in the canine coronary occlusion model. *Circulation*. 1998;98:2055–2064.
25. Kornowski R, Hong MK, Gepstein L, Goldstein S, Ellahham S, Ben-Haim SA, Leon MB. Preliminary animal and clinical experiences

Downloaded from http://circ.ahajournals.org/ by guest on July 29, 2011

using an electromechanical endocardial mapping procedure to distinguish infarcted from healthy myocardium. *Circulation*. 1998;98:1116–1124.
26. Smeets JL, Ben-Haim SA, Rodriguez LM, Timmermans C, Wellens HJ. New method for nonfluoroscopic endocardial mapping in humans: accuracy assessment and first clinical results. *Circulation.* 1998;97: 2426–2432.
27. Callans DJ, Ren JF, Michele J, Marchlinski FE, Dillon SM. Electroanatomic left ventricular mapping in the porcine model of healed anterior myocardial infarction: correlation with intracardiac echocardiography and pathological analysis. *Circulation*. 1999;100:1744–1750.
28. Marchlinski FE, Callans DJ, Gottlieb CD, Zado E. Linear ablation lesions for control of unmappable ventricular tachycardia in patients with ischemic and nonischemic cardiomyopathy. *Circulation*. 2000;101: 1288–1296.
29. Hsia HH, Callans DJ, Marchlinski FE. Characterization of endocardial electrophysiologic substrate in patients with nonischemic cardiomyopathy and monomorphic ventricular tachycardia. *Circulation*. 2003;108: 704–710.
30. Klein H, Karp RB, Kouchoukos NT, Zorn GL Jr, James TN, Waldo AL. Intraoperative electrophysiologic mapping of the ventricles during sinus rhythm in patients with a previous myocardial infarction: identification of the electrophysiologic substrate of ventricular arrhythmia. *Circulation*. 1982;66:847–854.
31. Cassidy DM, Vassallo JA, Miller JM, Poll DS, Buxton AE, Marchlinski FE, Josephson ME. Endocardial catheter mapping in patients in sinus rhythm: relationship to underlying heart disease and ventricular arrhythmias. *Circulation*. 1986;73:645–652.
32. Thiene G, Basso C. Arrhythmogenic right ventricular cardiomyopathy: an update. *Cardiovasc Pathol*. 2001;10:109–117.
33. Hisaoka T, Kawai S, Ohi H, Ishijima M, Okada R, Hayashida N, Saiki S, Kobayashi H, Yoshimura H. Two cases of chronic myocarditis mimicking arrhythmogenic right ventricular dysplasia. *Heart Vessels*. 1990; 5:51–54.
34. Hofmann R, Trappe HJ, Klein H, Kemnitz J. Chronic (or healed) myocarditis mimicking arrhythmogenic right ventricular dysplasia. *Eur Heart J*. 1993;14:717–720.
35. Winters GL, McManus BM: Myocarditis. In: Silver MD, Gotlieb AI, Schoen FJ, eds. *Cardiovascular Pathology*. Philadelphia, Pa: Churchill Livingstone; 2001.
36. Ott P, Marcus FI, Sobonya RE, Morady F, Knight BP, Fuenzalida CE. Cardiac sarcoidosis masquerading as right ventricular dysplasia. *Pacing Clin Electrophysiol*. 2003;26:1498–1503.
37. Dec GW, Fuster V. Medical progress: idiopathic dilated cardiomyopathy. *N Engl J Med*. 1994;331:1564–1575.
38. Fontaine G, Frank R, Tonet JL, Guiraudon G, Cabrol C, Chomette G, Grosgogeat Y. Arrhythmogenic right ventricular dysplasia: a clinical model for the study of chronic ventricular tachycardia. *Jpn Circ J*. 1984;48:515–538.
39. Turrini P, Angelini A, Thiene G, Buja G, Daliento L, Rizzoli G, Nava A. Late potentials and ventricular arrhythmias in arrhythmogenic right ventricular cardiomyopathy. *Am J Cardiol*. 1999;83:1214–1219.
40. Turrini P, Corrado D, Basso C, Nava A, Bauce B, Thiene G. Dispersion of ventricular depolarization-repolarization: a noninvasive marker for risk stratification in arrhythmogenic right ventricular cardiomyopathy. *Circulation*. 2001;103:3075–3080.

Downloaded from http://circ.ahajournals.org/ by guest on July 29, 2011